ARTICLE
Journal of Cellular Biochemistry 116:2528–2540 (2015)

Journal of Cellular Biochemistry

Association of Membrane/Lipid Rafts With the Platelet Cytoskeleton and the Caveolin PY14: Participation in the Adhesion Process

Doris Cerecedo,[1]* Ivette Martínez-Vieyra,[1] Deneb Maldonado-García,[2] Enrique Hernández-González,[2] and Steve J. Winder[3]

[1]*Laboratorio de Hematobiología, Escuela Nacional de Medicina y Homeopatía (ENMH), Instituto Politécnico Nacional (IPN), Mexico City, Mexico*

[2]*Departamento de Biología Celular, Centro de Investigación y de Estudios Avanzados del IPN (Cinvestav-IPN), Mexico City, Mexico*

[3]*Department of Biomedical Science, University of Sheffield, Sheffield, UK*

ABSTRACT

Platelets are the most prominent elements of blood tissue involved in hemostasis at sites of blood vessel injury. Platelet cytoskeleton is responsible for their shape modifications observed during activation and adhesion to the substratum; therefore the interactions between cytoskeleton and plasma membrane are critical to modulate blood platelet functions. Several cytoskeletal components and binding partners, as well as enzymes that regulate the cytoskeleton, localize to membrane/lipid rafts (MLR) and regulate lateral diffusion of membrane proteins and lipids. Resting, thrombin-activated, and adherent human platelets were processed for biochemical studies including western-blot and immunprecipitation assays and confocal analysis were performed to characterize the interaction of MLR with the main cytoskeleton elements and β-dystroglycan as well as with the association of caveolin-1 PY14 with focal adhesion proteins. We transfected a megakaryoblast cell line (Meg-01) to deplete β-dystroglycan, subsequent to their differentiation to the platelet progenitors. Our data showed a direct interaction of the MLR with cytoskeleton to regulate platelet shape, while an association of caveolin-1 PY14 with vinculin is needed to establish focal adhesions, which are modulated for β-dystroglycan. In conclusion, caveolin-1 PY14 in association with platelet cytoskeleton participate in focal adhesions dynamics. J. Cell. Biochem. 116: 2528–2540, 2015.

KEY WORDS: DYSTROGLYCAN; Meg-01 CELLS; CAVEOLIN-1; ADHERED PLATELETS

Platelets are small cell fragments derived from megakaryocytes that exhibit dramatic shape changes when they become activated. After exposure to several agonists, they go from a discoid shape, to a rounded shape with projecting filopodia, to a spread shape that facilitates efficient adhesion to the endothelium as well as to other platelets. The platelet cytoskeleton is responsible for these shape modifications and comprises microfilaments, a cortical coiled ring of microtubules, intermediate filaments, and associated proteins [Nachmias, 1980]. Assembly of actin filaments with actin-binding proteins determines the formation of specific structures developed during platelet activation including filopodia, lamellipodia, and focal adhesions. At the end of clot formation a contractile ring is involved in degranulation and platelet contraction [Bearer et al., 2002].

Cytoskeletal proteins in association with the plasma membrane establish several interactions that are essential for a wide variety of platelet processes such as cell shape and cell adhesion, cell motility and cell-cell contacts [Sechi and Wehland, 2000]. Signaling complexes formed by transmembrane and cytosolic proteins regulate these interactions and control important patterns that determine cell shape, as when bundled microfilaments span the cells and are anchored in the ventral plasma membrane in focal contacts. Focal contacts are enriched in a number of proteins, some of which are believed to play a role linking the actin cytoskeleton to the plasma membrane and to the extracellular

Grant sponsor: CONACYT-México; Grant number: 167178.

*Correspondence to: Dr. Doris A. Cerecedo Mercado, Laboratorio de Hematobiología, Escuela Nacional de Medicina y Homeopatía, I.P.N Guillermo Massieu Helguera No. 239, Col. La Escalera Ticomán, 07320 México, D.F México.
E-mail: dcereced@prodigy.net.mx

Manuscript Received: 18 November 2014; Manuscript Accepted: 14 April 2015
Accepted manuscript online in Wiley Online Library (wileyonlinelibrary.com): 17 June 2015
DOI 10.1002/jcb.25197 • © 2015 Wiley Periodicals, Inc.

matrix [Hagmann, 1993]. One example of a dual binding pattern protein is dystroglycan a ubiquitously expressed heterodimeric adhesion receptor which has a α-subunit connecting with the extracellular matrix while its transmembrane β-subunit connects to the actin filament network via cytoskeletal linkers including dystrophin, utrophin, ezrin, and plectin, depending on context. Dystroglycan was first described as part of the dystrophin glycoprotein complex of skeletal muscle; dystroglycan is an important adhesion molecule and signaling scaffold in several cell types and tissues [James et al., 2000; Ilsley et al., 2001; Ilsley et al., 2002].

Many plasma membrane proteins form clusters within lipid domains enriched in cholesterol and certain saturated acyl lipids, known as membrane or lipid rafts (MLR); their unique protein and lipid content make them structurally and functionally distinct and are critical for many cellular functions [Gonnord et al., 2012].

There are two major types of MLR: those that contain the cholesterol binding protein caveolin (Cav) and those that do not. Caveolin, is an integral membrane protein associated with the inner membrane leaflet that exists in 3 isoforms (Cav-1, -2, and -3) [Glenney, 1989]. Cav-1 is phosphorylated at Tyr14 in response to several mechanical stimuli and has also been linked to focal adhesion stability and dynamics, directional cell migration, ECM remodeling, caveolar endocytosis in response to specific stimuli and regulation of non-caveolar endocytic pathways [Joshi et al., 2012]. Caveolins can be phosphorylated by Src, Fyn, Yes, and c-Abl, certain growth factor receptors, and by integrin activation [Salanueva et al., 2007]. MLR containing caveolin form caveolae ("little caves"), flask-like invaginations of the plasma membrane while MLR that lack caveolin are flat structures. However, it is unclear why some cells express caveolin and contain lipid rafts do not have morphologically identifiable invaginated structures [Head and Insel, 2007].

Lipid rafts are also specific areas of membrane interacting with the cytoskeleton; in platelets this interaction is subjected to mechanical forces especially during clot retraction, in which integrins participate in the formation of a transmembrane linkage of proteins of extracellular matrix and form the actomyosin filament network [Bodin et al., 2005]. Moreover, in platelets the actomyosin cytoskeleton is involved in the lateral mobility of these micro-domains [Seveau et al., 2001] while cytoskeleton reorganization is needed to stabilize lipid raft clustering [Villalba et al., 2001].

Although the association between cytoskeletal components and MLR/caveolae had been previously described [Viola and Gupta, 2007; Simons and Gerl, 2010], the aim of the present study is to extend the notion that platelet cytoskeletal components can localize to MLR and act as platforms for cytoskeletal tethering and communication to the extracellular matrix (ECM) with a special focus in β-dystroglycan. Our results show that cholesterol is essential to modulate the platelet cytoskeleton reorganisation while the peculiar platelet structure help to resist total cholesterol depletion to maintain their key roles. Our results have also demonstrated, that the interactions of caveolin-1 PY14 with desmin and vinculin suggest that both actively participate during the adhesion process. The association of caveolin-1 PY14 with desmin contributes to the flexibility needed during platelet spreading; while its association with vinculin involves its participation in focal adhesion contacts.

Additionally we evaluated the participation of β-dystroglycan as a key scaffold component for caveolin-1 and focal adhesion kinase (FAK).

MATERIALS AND METHODS

EXPERIMENTAL DESIGN

To assess the thrombin effects on membrane raft assembly, resting and thrombin-activated platelets were processed for raft isolation procedures using sucrose gradients and ultracentrifugation. Raft markers (caveolin-1 and flotilin-1) were identified by western-blot assays in the 9 fractions obtained.

To establish the potential participation of cytoskeletal proteins (actin-filaments, intermediate filaments, and microtubules) in raft assembly, we identified them by western-blot in raft fractions, while its association with caveolin-1 were analyzed by confocal microscope from control and thrombin-activated platelets. To determine the association of caveolin-1 PY14 with the three main cytoskeleton proteins in platelet structures related to adhesion, we performed confocal analysis in adhered platelets; this association was corroborated in suspended and adhered platelets processed for immunoprecipitation assays with caveolin-1 PY14. To explore the feasible participation of caveolin-1 PY14 in focal adhesions immunoflourescence staining was performed using focal adhesion proteins such as vinculin, talin, and α-actinin.

To determine whether β-dystroglycan (β-Dg) a cytoskeleton protein co-fractionated with rafts, Wb of nine fractions of resting and thrombin-activated platelets were performed, evaluating its participation in adherent platelets associated with caveolin-1, by confocal and immunoprecipitation analysis. To evaluate the role of β-Dg for caveolae stability, we down-regulated the expression of β-Dg with an shRNA and by immunofluorescence, Wb and qRT-PCR demonstrated the up-regulation of proteins related with adhesion process.

PLATELET PREPARATION

Platelets were obtained by venopuncture from healthy donors who had not received any drug during the 10 days prior to sampling and who gave consent for the procedure to be carried out. Blood was immediately mixed with citrate anticoagulant including dextrose at pH 6.5 (93 mM sodium citrate, 70 mM citric acid, and 140 mM dextrose) at a blood:anticoagulant ratio of 9:1. Platelet-rich plasma was obtained from total blood by centrifugation at 100 *g* for 20 min at room temperature, and was subsequently mixed with an equal volume of citrate anticoagulant and centrifuged at 400 *g* for 10 min [White, 1983]. The platelet pack was suspended and washed twice with Hank's balanced saline solution (HBSS) without calcium (137 mM NaCl, 5.3 mM KCl, 1 mM $MgCl_2$, 0.28 mM $Na_2HPO_4.12H_2O$, 0.87 mM NaH_2PO_4, 0.44 mM KH_2PO_4, 4.1 mM $NaHCO_3$, and 5.5 mM glucose) and counted in a hematocytometer.

ANTIBODIES USED

Caveolin-1 polyclonal antibody (pAb) Catalogue Cat. no. sc-53564, actin monoclonal antibody (mAb) no. sc-8432, α-tubulin mAb Cat no. sc-5286, Cav 1 PY14 pAb Cat. no. sc-101653, β-dystroglycan

pAb Cat. no. sc-30405, vimentin pAb Cat. no. sc-7557, Focal adhesion kinase (FAK) Cat. no. sc-557, integrin β-1 Cat. no. sc-8978, α-actinin Cat. no. sc-7454, talin Cat. no. sc-7534, vinculin Cat. no. sc-7649 were purchased from Santa Cruz Biotechnology, Inc. (Santa Cruz, CA).

IMMUNOFLUORESCENCE ASSAYS

Fixed resting, thrombin-activated platelets treated with 10 mM MβCD were allowed to adhere to glass cover slips in a humid camera for 20 min. Non-fixed resting control platelets and platelets treated with 10 mM MβCD were adhered to glass cover slips in a humid camera for 20 min, non-adherent cells were removed by washing with HBSS, fixed, and permeabilized with a mixture of 2% p-formaldehyde and 0.04% NP40 in PHEM solution (100 mM PIPES, 5.25 mM HEPES, 10 mM EGTA, and 20 mM $MgCl_2$). Platelets were incubated first with the specific primary antibodies diluted in PBS 0.1% bovine serum albumin for 2 h. Cells were washed with PHEM solution and incubated for 1 h with secondary antibody conjugated to Alexa-Fluor-488 or Alexa-Fluor-568 (Molecular Probes, Life Technologies Grand Island, NY) and then washed several times with PHEM and mounted in Vectashield (Vector Laboratories, Inc., Burlingame, CA). Slides were observed using a Leica confocal instrument model TCS-SP5 Mo, lasers were configured to 20% (17% outside) for Argon and 45% for He/Ne 543, and images were taken at 63× zoom 7× at 1024 × 1024 pixels with an HCX PL APO 63 · /1.40–0.60 DIL CS oil immersion. Optical sections (z) were performed at 118 nm with one Airy unit. Negative controls included cells incubated with an irrelevant polyclonal antibody and slides were only exposed to secondary antibodies conjugated to the fluorochromes. Likewise, platelets incubated with 0.1% DMSO were processed for 1 h as the solvent control.

For cholesterol staining with filipin, suspended, thrombin-activated, or adherent fixed platelets were incubated with 1 ml of 1.5 mg glycine/ml PBS for 10 min at room temperature to quench the paraformaldehyde before they were stained with 1 ml of filipin working solution for 2 h at room temperature. After rinsing with PBS they were analyzed with confocal microscope using a UV filter set (340–380 nm excitation, 40 nm dichroic, 430–nm long pass filter).

WESTERN BLOTTING

Lysates from resting and adherent platelets obtained in sodium dodecyl sulfate (SDS) and β-mercaptoethanol were boiled for 5 min, subjected to 10% SDS–Polyacrylamide gel electrophoresis (PAGE), and transferred onto nitrocellulose membranes using a semi-dry system (Thermo Electron Co., Milford, MA). Membranes were incubated with appropriate primary antibodies, then with Horseradish peroxidase (HRP)-conjugated secondary antibodies visualized using an enhanced chemoluminescence western blotting analysis system (Santa Cruz Biotechnology, Inc.), and documented using T-mat G/RA film (Kodak, Rochester, NY). Negative controls comprised transferred strips incubated solely with HRP-conjugated secondary antibodies.

IMMUNOPRECIPITATION ASSAYS

Resting and adherent platelets were lysed for 15 min at 4°C with an equal volume of 2× lysis buffer (2 mM EGTA, 100 mM HEPES, 150 mM NaCl, and 2% NP40, pH 7.4) containing a protease inhibitor cocktail. Lysates were incubated for 2 h at 4°C with the immunoprecipitating antibodies and subsequently incubated overnight with Protein G-Sepharose (Santa Cruz Biotechnology, Santa Cruz, CA). Immunoprecipitates (Ip) were separated by centrifugation and washed with NP40-free lysis buffer, then re-suspended in 2× sample buffer (125 mM Tris-HCl, 4% SDS, 20% glycerol, 0.01 mg/ml β-mercaptoethanol and bromophenol blue, pH 6.8) and boiled for 5 min. Immunoprecipitated proteins (Ip) and supernatants were analyzed by western blotting.

RAFT ISOLATION PROCEDURES

Platelets (1.5×10^9 in 750 μl) were lysed by addition of 250 μl ice-cold 4°C buffer [2% Triton X-100 (v/v), 150 mM NaCl, 100 mM Mes, pH 6.5, 3 mM PMSF, 3 mM Na3VO4, 8 μg/ml each of leupeptin and aprotinin] and incubated for 5 min. Procedures were performed at 4°C as described [Bodin et al., 2001]. The 1.5 ml lysate was adjusted to 1.37 M (40%) sucrose by addition of 1 ml of 2.74 M sucrose prepared in Mes-buffered saline (MBS) (150 mM NaCl, 25 mM Mes, pH 6.5, 1 mM PMSF, 1 mM Na_3VO_4). A step sucrose gradient was made by successive additions of 1 M (30%), 0.8 M (25%), 0.6 M (20%), 0.5 M (15%), 0.3 M (10%), 0.15 M (5%) sucrose solution (1.33 ml each) on the top of the 1.37 M (40%) homogenate. The gradients were ultracentrifuged (200,000 *g*, 4°C, 16 h) and nine fractions of equal volume were harvested from the top by pipetting.

MEG-01 CELL CULTURE AND DIFFERENTIATION

Meg-01 cells were cultured in RPMI-1640 medium supplemented with 10% fetal bovine serum, 400 mM L-glutamine, 50 lM gentamicin, 25 mM HEPES, 2 g/L sodium bicarbonate, 1 mM sodium pyruvate in a humid atmosphere of 5% CO_2 at 37°C. For differentiation into a megakaryocte phenotype, Meg-01 cells (diffMeg) were differentiated with I 2-0-tetradecanoylphorbol- I 3-acetate (TPA) 10^{-7} M for 7 days [Ogura et al., 1988]. Cell viability was assessed by exclusion of 0.2% trypan blue and was routinely >90% before and after differentiation.

PLASMIDS AND TRANSFECTION

shRNA constructs targeting dystroglycan or control shRNA were generated using the RNAi- Ready pSiren-RetroQ system (Clontech Laboratories) have been described previously [Mitchell et al., 2013]. Meg-01 cells (2×10^6/ml) were transfected with 2 μg DNA mixed with 2 μg pEGFP-N1 to mark the shRNA transfected cell population (Clon-Tech, Mountain View, CA) using a Nucleofector II (Amaxa), according to the manufacturer's recommendation (Lonza Walkerrsville Inc. Walkersville, MD). Twenty-four hours after transfection cells were selected. For functional assays, selected cells were differentiated for 7 days.

RNA ISOLATION

RNA was isolated from Meg-01 cells using TRIzol® LS Reagent (Ambion, Life Technologies Corp., Carlsbad, CA), and disolved in 25 μl of ultrapure water The quantity of RNA was measured using a spectrophotometer (NanoDrop 2000c; Thermo Scientific, Inc). Samples with the RNA concentration (A260/A280 ≥1.8 ng/μl) and purity (A230/A260 ≥2.0 ng/μl) were selected.

QUANTITATIVE REVERSE TRANSCRIPTION PCR (QRT-PCR)

qRT-PCR was performed using KAPA SYBR FAST One Step qRT-PCR kit (Kapa Biosystems INC, Wilmington, MA). Primers for Caveolin-1 forward (5′-GAGCGAGAAGCAAGTGTACGA-3) and reverse (5′-ACAGACGGTGTGGACGAAGAT-3′); FAK forward (5′-CGCT-GGCTGGAAAAAGAGGAA-3′) and reverse (5′-TCGGTGGGT-GCTGGCTGGTAGG-3′) and GAPDH. PCRs were performed in a 10 μl total reaction volume in a Step One Real Time PCR system (Applied Byosistems Foster City, CA). An initial cycle step at 95°C for 5 min was followed by 40 cycles with a 12 s denaturation at 95°C, 12 s annealing with a temperature of 64°C, followed by 12 s primer extension at 72°C, finally by 15 s at 95°C to ensure complete extension. 1 min at 60°C and 15 s at 95°C, to generate a melt curve. PCR products were visualized by means of a 1.0% (w/v) agarose gel containing ethidium bromide. Three biological replicates of Control RNAi and Dg RNAi were examined. The comparative CT (ΔΔCT) method was selected to determine the amount of target nucleic acid sequence in each sample relative to the control samples.

STATISTICAL ANALYSIS

Statistical analysis was carried out with the GraphPad Prism for Windows version 5 (GraphPad Software, Inc. La Jolla, CA). One-way Analysis of variance (ANOVA) with a multiple comparison test (Tukey test) was utilized for Western-blot analysis. Relative protein expression, relative immunofluorescence expression and relative mRNA expression were analyzed with unpaired *t*-student. Statistical significance was defined as $P < 0.05$.

RESULTS

CHOLESTEROL IS RETAINED IN THE PLATELET MEMBRANOUS SYSTEM

Lipid raft microdomains are characterized by their insoluble nature in non-ionic detergents as well as the presence of glycosphingo-lipids, gangliosides, and sterols. We first investigated whether thrombin affects membrane raft assembly or raft coalescence in platelets by assessing changes in membrane fraction distribution of caveolin-1 and flotilin-1 after thrombin stimulation. In resting control conditions caveolin-1 was found in fractions 2, 3, 8, and 9 (Fig. 1A), while in thrombin-activated platelets caveolin-1 was mainly observed in the first 3 fractions (Fig. 1A). Similarly, flotilin-1 was found in fractions 1, 2, 7, 8, and 9 in resting platelets (Fig. 1B), and mostly in fractions 1-4 in thrombin-activated platelets (Fig. 1B).

To verify that the detergent insoluble fractions represented lipid rafts, cells were treated with methyl-β-cyclodextrin (MβCD), a known membrane cholesterol-chelating agent. Following MβCD treatment, raft integrity was examined by membrane partitioning of caveolin-1 and flotilin-1 (Fig. 1C and D, respectively). In resting conditions, treatment with MβCD abrogated partitioning into the detergent-insoluble membrane fraction of caveolin-1 with a lesser extent for flotilin-1, which was also present in low-density fractions (Fig. 1C and D), consistent with lipid raft distribution. In thrombin-activated fractions, caveolin-1 distribution was not affected compared to control (Fig. 1B). Flotilin-1 diminished its distribution in low-density fractions but was clearly present in fraction 1 (Fig. 1D). Densitometry analysis of respective Wb was performed and is resumed in Supplemental Figure 1.

To assess the presence of residual cholesterol in the inner membranous system of control and MβCD treated resting, thrombin-activated and adherent platelets, we used filipin as it binds to cholesterol with high affinity [Castanho et al., 1992]. Platelets have two discrete membrane systems not found in other blood cells: the open canalicular system (OCS), and the dense tubular system (DTS) with no apparent physical communication between them and restricted to one or two areas of the cytoplasm [White, 1999], in adhered platelets these systems as well as the granules are observed at the center of the platelet named granulomere zone. Resting control platelets were observed with a label of filipin at the plasma membrane and inner membranous system, while in thrombin activated platelets filipin was mainly present at the granulomere zone. Control adhered platelets showed the presence of cholesterol with a punctuate pattern at the granulomere zone (white circle) with relatively little at the plasma membrane (Fig. 1E). Resting and thrombin-activated platelets incubated with MβCD conserved the filipin staining at the center of the platelet. In adhered platelets the filipin-staining pattern was consistent with the presence of cholesterol in the cytoplasm corresponding to the granulomere zone and short filopodia of the cells (Fig. 1F arrow and arrowheads respectively).

ACTIN AND TUBULIN ARE ASSOCIATED WITH RAFTS IN RESTING AND THROMBIN-ACTIVATED HUMAN PLATELETS

In human platelets, lipid rafts co-isolate with actin [Bodin et al., 2005] and there is a close association between actin, intermediate filaments, and microtubules [Cerecedo et al., 2013] so it was important to determine if intermediate filaments and microtubules were also associated with lipid rafts. We therefore treated cells with MβCD and examined actin, desmin, and tubulin partitioning in membrane fractions of resting and thrombin-activated platelets.

For control resting and thrombin-activated platelets actin, but not desmin or tubulin was observed at low-density fractions of the gradient (Fig. 2A). Actin and tubulin were recovered from low-density fractions of resting platelets treated with MβCD (Fig. 2B), however, in thrombin-activated MβCD treated platelets actin was observed in high-density fractions, tubulin was present with a faint band in fraction 1 (Fig. 2B). Densitometry analysis of respective Wb was performed and is resumed in Supplemental Figure 2.

In order to reveal the subcellular distribution of caveolin-1 in resting, thrombin-activated and adherent platelets, we assayed double immunofluorescence staining utilizing an antibody raised against caveolin-1 and either TRITC-phalloidin to stain F-actin or antibodies to α-tubulin or desmin to stain microtubules or intermediate filaments respectively. Suspended and adhered platelets treated with MβCD were also processed for immunofluorescence staining of caveolin-1 with actin, tubulin, or desmin. Confocal analysis showed that in platelets in suspension, Caveolin-1 was distributed in discrete patches around the plasma membrane and in the cytoplasm (Fig. 2Ci); in thrombin-activated platelets (Fig. 2Cii) the signal remained at the plasma membrane and was also distributed in filopodia with F-actin. In adhered platelets (Fig. 2Ciii), the pattern of Caveolin-1 patches was conserved at the plasma

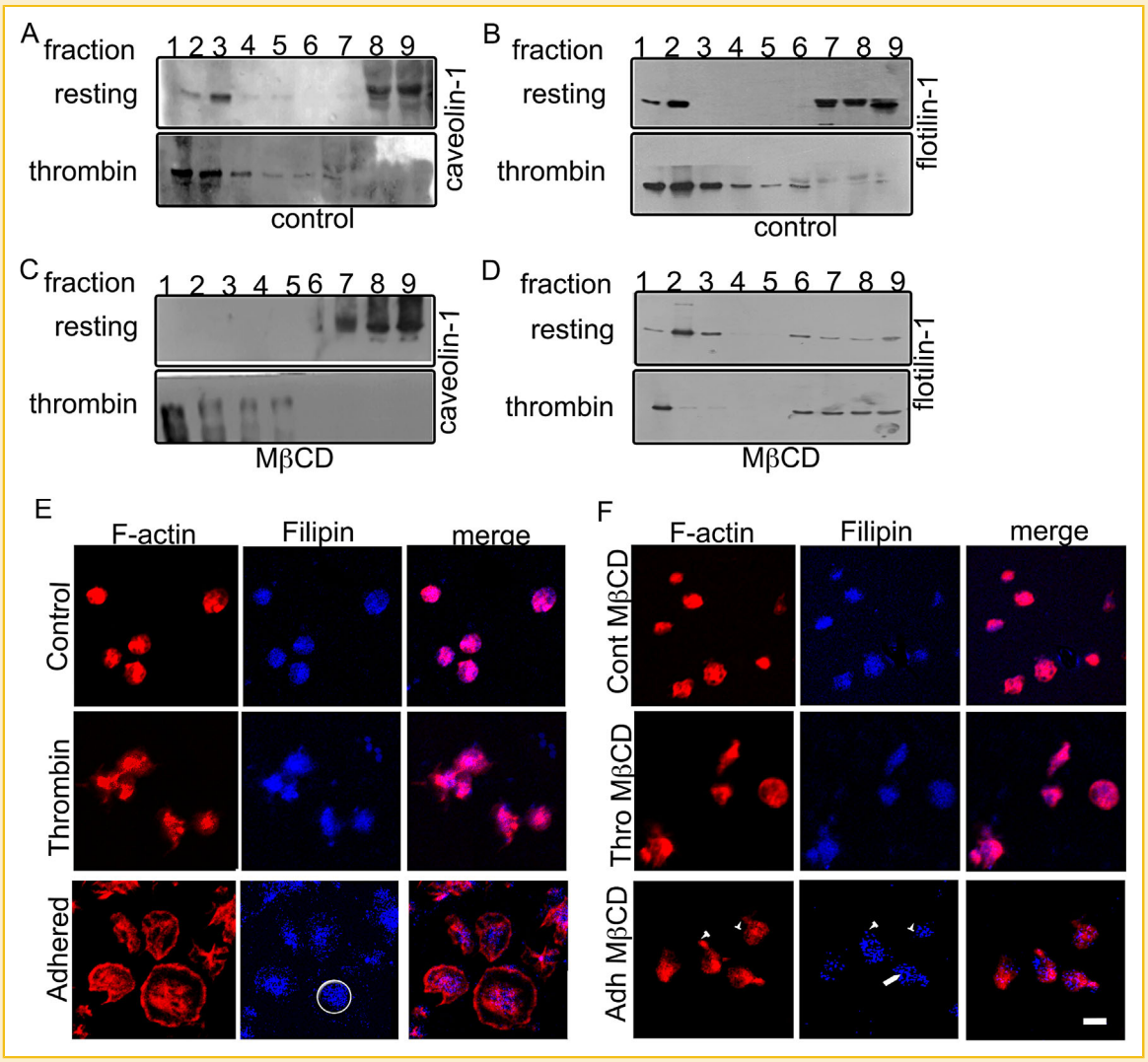

Fig. 1. Cholesterol pools were retained at the Open canalicular system (OCS). Panel A. Distribution of the raft marker protein caveolin-1 in nine fractions of a 5–30% discontinuous sucrose gradient containing 1% Triton X-100 lysates from control resting or thrombin-activated platelets. Fraction 1 is lightest and fraction 9 is densest. (n = three independent experiments). Panel B. Distribution of the raft marker protein flotilin-1 in the nine fractions of the sucrose gradient fractions containing 1% Triton X-100 lysates from control resting or thrombin-activated platelets. (n = three independent experiments). Panel C. Distribution of the raft marker protein flotilin-1 in sucrose gradient fractions containing 1% Triton X-100 lysates from MβCD resting or thrombin-activated platelets. (n=three independent experiments). Panel D. Distribution of the raft marker protein flotilin-1 in sucrose gradient fractions containing 1% Triton X-100 lysates from MβCD treated resting or thrombin-activated platelets. Results are representative of three independent experiments. Panel E. Confocal analysis of control and MβCD-treated resting, thrombin-activated and adherent platelets stained with filipin (blue) and phalloidin labelled with Tetramethyl rhodamine iso-thiocyanate (TRITC). The respective merged images are shown. White circle indicates the granulomere zone, arrowheads indicate filopodia. (n = three independent experiments). Scale bar = 1.5 μm.

membrane and concentrated in the cytoplasm particularly in the region in which the granules were centralized (granulomere). In resting platelets, F-actin was observed in clusters around the platelet, desmin was observed as cytoplasmic thick aggregates; while microtubules were organized as rings around the periphery of the platelet (Fig. 2Ci). Thrombin-activated platelets maintained the original distribution of the three-cytoskeleton elements, but they were also found redistributed to filopodia (Fig. 2Cii). By contrast the adhesion process triggers dramatic changes to the three-cytoskeleton elements. F-actin is reorganized into bundles radiating from the granulomere zone to the leading edge of the plasma membrane, microtubules were fragmented and redistributed through the cytoplasm as thick radiating bundles, and desmin was observed at the cytoplasm and plasma membrane (Fig. 2Ciii). Merged images between caveolin-1 and the cytoskeleton elements showed co-localization with F-actin and tubulin at the plasma membrane of resting platelets (Fig. 2 Ci); with desmin and tubulin in thrombin-activated platelets (Fig. 2 Cii) and with F-actin and desmin at the granulomere zone of adhered platelets (Fig. 2Ciii). MβCD disturbed the patched distribution of caveolin-1 in resting platelets with the labelling distributed more around the plasma membrane (Fig. 2Di); while in thrombin-activated platelets, caveolin-1 was

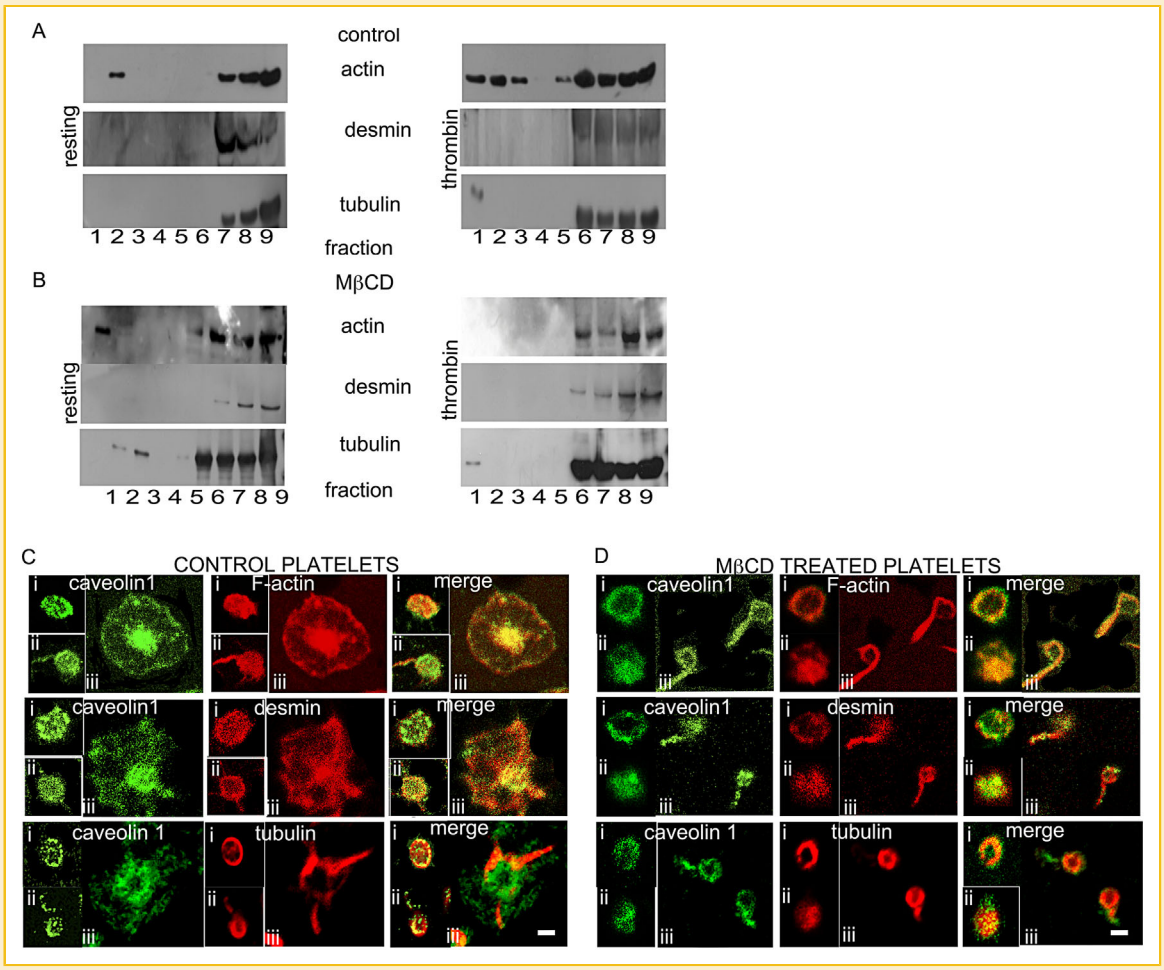

Fig. 2. Cytoskeleton proteins are associated with rafts in resting and thrombin-activated human platelets. Panel A. 1% Triton X-100 lysates of control resting and thrombin-activated human platelets were subjected to a flotation assay in a sucrose gradient. Fractions of the sucrose gradient were resolved by Western-blot and analyzed using antibodies against actin, desmin, and tubulin. Blots are representative of three independent experiments. Panel B. 1% Triton X-100 lysates of resting and thrombin-activated human platelets treated with MβCD were subjected to a flotation assay in a sucrose gradient. Fractions of the sucrose gradient were resolved by Western-blot and analyzed using antibodies against actin, desmin, and tubulin. Blots are representative of three independent experiments. Panel C. Control resting (Ci), thrombin-activated (Cii) and platelets settled on glass for 20 min (Ciii) were analyzed by confocal microscopy after processing for double-labelling using antibodies directed against caveolin-1 identified with secondary antibodies labelled with Fluorescein iso-thiocyanate (FITC) and phalloidin labelled with Tetramethyl rhodamine iso-thiocyanate (TRITC), and antibodies directed against desmin and α-tubulin revealed with secondary antibodies conjugated to Alexa-Fluor-568. The respective merged images are shown. Scale bar = 1.5 μm. (n = three independent experiments). Panel D. MβCD-treated resting (Di) thrombin-activated (Dii) and platelets settled on glass for 20 min (Diii) were analyzed by confocal microscopy for caveolin-1, F-actin, desmin ,and α-tubulin as in C. The respective merged images are shown. Scale bar = 1.5 μm. (n = three independent experiments).

homogeneously distributed at the cytoplasm and the filopodia were absent (Fig. 2Dii). Actin, desmin and tubulin were also disturbed and remained around the plasma membrane of resting platelets (Fig. 2Di) while in thrombin-activated platelets the three-cytoskeleton elements were observed mainly in the cytoplasm (Fig. 2Dii). Caveolin-1 co-localized with actin filaments, desmin, and tubulin at the plasma membrane and at the cytoplasm of resting (Fig. 2Di) and thrombin-activated platelets treated with MβCD (Fig. 2Dii). Treatment with MβCD prevented full platelet spreading (Fig. 2Diii); most of the platelets observed under this condition elongated the membrane as a long thick filopodia concentrating the presence of Caveolin-1 around the plasma membrane as patches. Not fully extended platelets maintained F-actin, microtubules, and desmin at the plasma membrane. A strong co-localization of Caveolin-1 was observed only with actin filaments in adherent MβCD treated platelets (Fig. 2Diii).

THE PHOSPHORYLATED FORM OF CAVEOLIN-1 ASSOCIATES WITH INTERMEDIATE FILAMENTS IN ADHERED PLATELETS

Having found a feasible association between caveolin-1 and cytoskeleton proteins, we wanted to determine the distribution of caveolin-1 phosphorylated on tyrosine 14 (PY14) a common post-translational modification [Li et al., 1996] in adhered platelets. Therefore we processed adherent platelets for double

immnofluorescence staining with F-actin, tubulin, and desmin to be analyzed by confocal microscopy as described above.

The tyrosine-phosphorylated form of caveolin-1 (Cav-1 PY14) was found at the plasma membrane and in the cytoplasm of resting platelets (Fig. 3A insets); while in adherent platelets its distribution was observed at the tips of filopodia (arrowheads) and in the cytoplasm. A punctuate pattern was also very evident at the plasma membrane and at the granulomere zone of fully adhered platelets (Fig. 3A). Cav-1 PY14 was co-localized with actin filaments, desmin, and tubulin in resting and adherent platelets. The presence of Caveolin-1 PY14 with a patched pattern at the plasma membrane and filopodia strongly suggested its association with focal adhesions (arrowheads). To quantify caveolin-1 PY14 expression in resting, adhered and thrombin-activated platelets, densitometry analysis of Wb bands was performed. Caveolin-1 in its tyrosine phosphorylated form was observed in all the conditions assayed but mainly in thrombin-activated platelets (Fig. 3B), although the difference was not statistically significant.

To ascertain whether caveolin-1 PY14 was associated with cytoskeleton proteins, immunoprecipitations with caveolin-1 PY14 antibody were processed from extracts of resting and adherent platelets. The immunoprecipitation of caveolin-1 PY14 from resting platelets pulled down actin in resting conditions and desmin in adhered platelets, while tubulin did not associate with caveolin-1 PY14 in either condition.

CAVEOLIN-1 PY14 PARTICIPATES IN FOCAL ADHESION COMPLEX IN HUMAN PLATELETS

Since the distribution of caveolin-1 PY14 was observed in adherent platelets as patches that may represent focal contacts, double immunoflourescence staining was performed using anti-caveolin PY14 and candidate focal adhesion proteins such as vinculin, talin, and α-actinin.

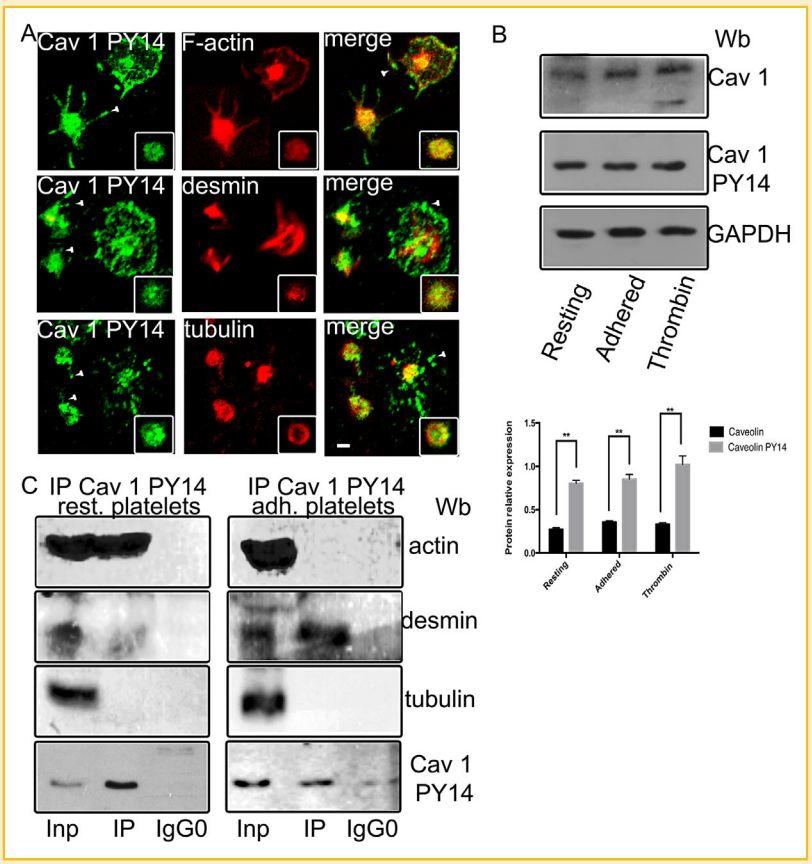

Fig. 3. The phosphorylated form of caveloin-1 is present at filopodia and associates with intermediate filaments in adhered platelets. Panel A. Control resting (bottom inset) and platelets settled on glass for 20 min were analyzed by confocal microscopy after processing for double-labeling using antibodies directed against caveolin-1 identified with secondary antibodies labeled with Fluorescein iso-thiocyanate (FITC) and phalloidin labeled with Tetramethyl rhodamine iso-thiocyanate (TRITC), and antibodies directed against desmin and α-tubulin were revealed with secondary antibodies conjugated to Alexa-Fluor-568. The respective merged images are shown. Scale bar = 1.5 μm. (n = three independent experiments). Panel B. Total platelet lysates were analyzed by Western blot utilising antibodies against Caveolin-1 and caveolin-1 phosphorylated (Cav 1 PY14). Quantitative analysis using GAPDH as loading control was used. Values shown are mean ± SEM from three independent experiments (n = 3), respectively. ** $P = <0.05$. Panel C. Control resting and platelets adherent to glass for 20 min were processed for immunoprecipitation assays using the anti-Caveolin-1 PY14 antibody (IP). Proteins from total Extracts (Inp) and Immunoprecipitates (IP) were analyzed by immunoblot utilizing antibodies against actin, desmin, α-tubulin, and Caveolin-1 PY14. Bands corresponding to actin, desmin, α-tubulin, and Caveolin-1 PY14 were detected. None of these proteins were detected in control IgG immunoprecipitates (IgG0 lane). (n = three independent experiments).

In full-extended platelets, vinculin intensely stained the granulomere zone, and showed a submembrane punctuate distribution at the plasma membrane, while talin was located with a dispersed labeling of the granulomere zone, but more homogeneously at the lamellipodia (Fig. 4A). α-actinin showed a more diffuse cytoplasmic staining with very little distribution at the plasma membrane (Fig. 4A). Vinculin appeared colocalising with caveolin-1 PY14, both in peripheral patches and in the granulomere.

To corroborate the data observed by confocal analysis, we performed immunoprecipitation assays from resting, and fully adhered platelet extracts using a caveolin-1 PY14 antibody. Total lysate input (Inp) and immunoprecipitation extracts (Ip) were resolved by western blot using antibodies directed against integrin β-1, vinculin, talin, α-actinin, and focal adhesion kinase (FAK) (Fig. 4B). The results demonstrated that the only specific observable interaction, in either resting or adherent platelet extracts, was between caveolin-1 PY14 and vinculin, with a noticeably stronger interaction in adhered platelets. These data suggest that caveolin-1 PY14 interacts with focal adhesion complexes through an association with vinculin in adhered platelets.

B-DYSTROGLYCAN CO-FRACTIONATES AND CO-PRECIPITATES WITH CAVEOLIN-1

We have reported the association of β-dystroglycan (β-Dg) an abundant transmembrane protein in human platelets [Cerecedo et al., 2005], with proteins involved in focal adhesions including vinculin [Cerecedo et al., 2008]. In addition, it has been reported the association between caveolin-1 and β-dystroglycan [Sharma et al., 2010], therefore we wanted to determine whether β-dystroglycan and caveolae share cellular domains using sucrose density gradient ultracentrifugation for fractionation of control or MβCD-treated human platelets. β-dystroglycan co-fractionates (Fig. 5A) in caveolin-1- and flotilin-1 enriched microdomains of resting platelets (Fig. 1A and B), but not in thrombin-activated or platelets treated with MβCD. Densitometry analysis of respective Wb was performed and is resumed in Supplemental Figure 3. We next used double immunofluorescence staining utilizing an antibody raised against Caveolin-1 and anti-β-dystroglycan in resting, thrombin-activated (Fig. 5Bi,Bii) and adherent platelets treated or not with MβCD (Fig. 5Biii). β-dystroglycan was located at the plasma membrane of resting platelets while in thrombin-activated platelets the label was distributed to the cytoplasm; its co-localisation with caveolin-1 was observed at the plasma membrane in resting and activated control and MβCD platelets. In adherent platelets β-dystroglycan was found at the plasma membrane, in filopodia and in structures reminiscent of stress fibres, and co-localizing with caveolin-1 at the plasma membrane and granulomere zone. In adherent platelets treated with MβCD; the colocalisation was observed at the cytoplasm and incipient filopodia.

To corroborate whether β-dystroglycan and caveolin-1 interacted, we performed immunoprecipitation of resting and adherent platelets, and we found that these proteins co-precipitated in presence of the antibody against β-dystroglycan and the complementary experiment using anti-caveolin-1 (Fig. 5C).

To determine if β-dystroglycan was distributed in remaining cholesterol compartments, we performed double inmunostaining, labeling β-dystroglycan and cholesterol with filipin in resting (bottom insets) and adherent control platelets and in adherent MβCD-treated platelets. Cholesterol and β-dystroglycan overlapped at the cytoplasm of resting platelets (Fig. 5D, right top inset), in control adherent platelets the overlap was observed at the

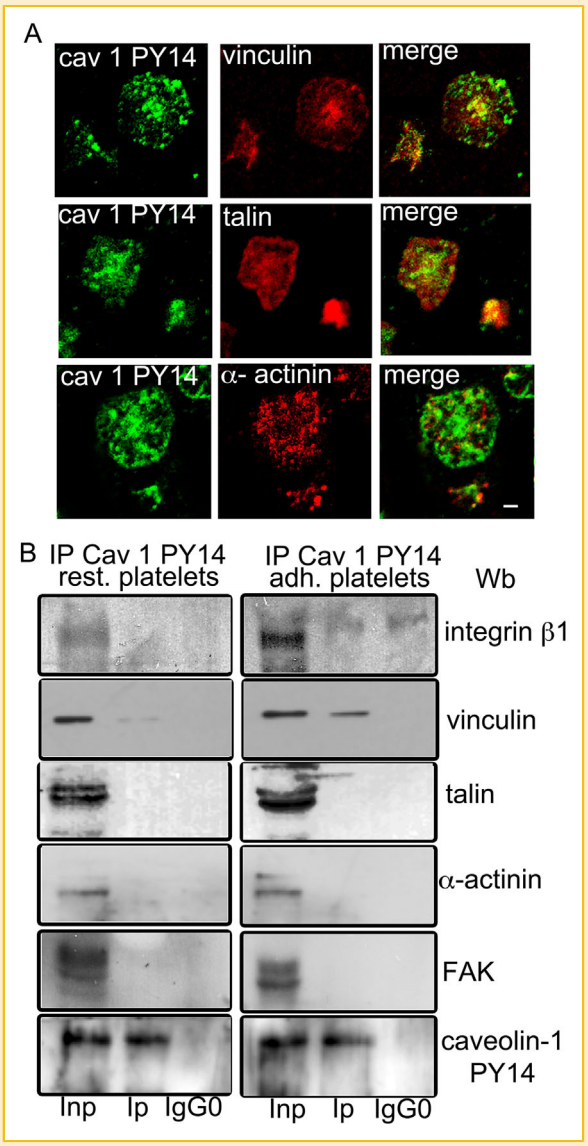

Fig. 4. Caveolin-1 PY14 participates in focal adhesion complex in human platelets. Panel A. Platelets settled on glass for 20 min were analyzed by confocal microscopy after processing for double-labelling using antibodies directed against caveolin-1 PY14 identified with secondary antibodies labelled with Fluorescein iso-thiocyanate (FITC) and antibodies directed against vinculin, talin, and α-actinin revealed with secondary antibodies conjugated to Alexa-Fluor-568. The respective merged images are shown. Scale bar = 1.5 μm. (n = three independent experiments). Panel B. Resting and platelets adherent to glass for 20 min were processed for immunoprecipitation assays using the anti-Caveolin-1 PY14 antibody (IP). Proteins from total Extracts (Inp) and Immunoprecipitates (Ip) were analyzed by immunoblot utilizing antibodies against integrin β-1, vinculin, talin, α-actinin, FAK, and Caveolin-1 PY14. Bands corresponding to integrin β-1, vinculin, talin, α-actinin, FAK, and Caveolin-1 PY14 were detected. None of these proteins were detected in control IgG immunoprecipitates (IgG0 lane). (n = three independent experiments).

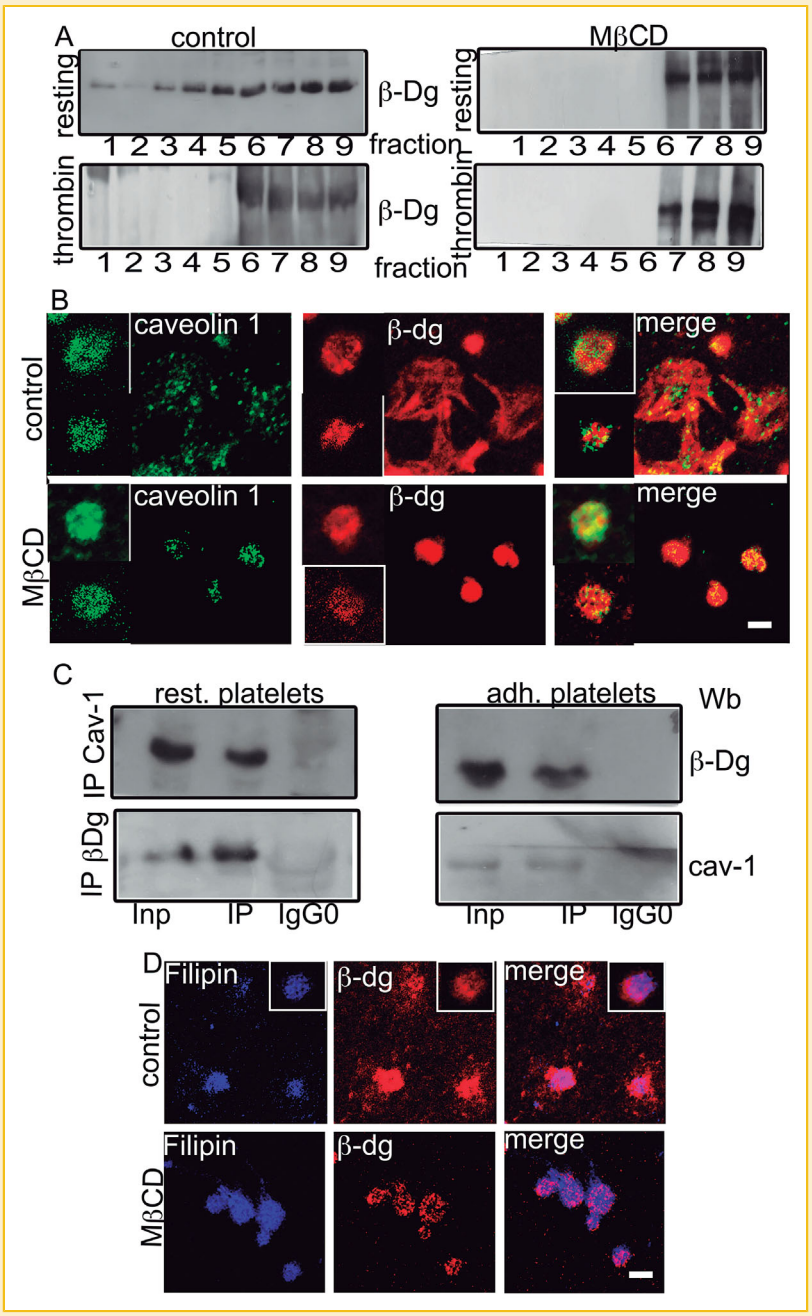

Fig. 5. β-Dystroglycan co-fractionates and co-precipitates with caveolin-1. Panel A. Control and MβCD-treated platelets were lysed in 1% Triton X-100 for isolation of caveolae enriched by sucrose density gradient centrifugation. Equal amounts of protein from each fraction were subjected to protein blot analysis for β-dystroglycan (β-Dg). Results are representative of three independent experiments. Panel B. Control and MβCD resting (Bi), thrombin-activated (Bii), and platelets settled on glass for 20 min (Biii) were analyzed by confocal microscopy after processing for double-labelling using an antibody directed against caveolin-1 identified with a secondary antibody labeled with Fluorescein iso-thiocyanate (FITC) and an antibody directed against β-dystroglycan (β-Dg) revealed with a secondary antibody conjugated to Alexa-Fluor-568. The respective merged images are shown. Scale bar = 1.5 μm. Results are representative of three independent experiments. Panel C. Control and MβCD-treated resting and platelets adherent to glass for 20 min were processed for immunoprecipitation assays using the anti-Caveolin-1 and β-dystroglycan (β-dg) antibody (IP). Proteins from total Extracts (Inp) and Immunoprecipitates (IP) were analyzed by immunoblot utilizing antibodies against β-dystroglycan (β-Dg), and Caveolin-1. Bands corresponding to β-dystroglycan (β-Dg), and Caveolin-1 were detected. None of these proteins were detected in control IgG immunoprecipitates (IgG0 lane). (n = three independent experiments). Panel D. Confocal analysis of control adherent platelets and MβCD treated adherent platelets stained with filipin and an antibody directed against β-dystroglycan (β-Dg) labeled with a secondary antibody conjugated to Alexa-Fluor-568. The respective merged images are shown. Scale bar = 1.5 μm. Results are representative of three independent experiments.

granulomere zone, while in adherent MβCD-treated platelets cholesterol and β-dystroglycan merged at the centre of the platelet (Fig. 5D).

B-DYSTROGLYCAN IS NEEDED TO MODULATE FOCAL ADHESION CONTACTS

As our data indicated that caveolin-1 is associated with β-dystroglycan, we assessed weather β-dystrolgycan was essential for caveolae integrity and focal adhesions. To address this, we transfected and differentiated Meg-01 cell line to megakaryocytic lineage (platelets precursors) using a small interfering RNA (RNAi) to target dystroglycan (Dg RNAi). The RNAi was co-expressed with GFP to identify unequivocally individual RNAi-treated cells. As negative control, RNAi that is predicted not to block the translation of any specific gene was utilized (control RNAi). Effectiveness of RNAi treatment in reducing β-dystroglycan expression in these cells was evaluated by western blotting and immunofluorescence assays. Global immunolabeling of β-dystroglycan was reduced by more than 50% in GFP-expressing cells that co-express Dg specific RNAi, compared with control RNAi-treated cells (Supplemental Fig. 4). These levels of knock down are in keeping with studies in other cell lines using the same targeting sequences [Martinez-Zarate et al., 2014]. To determine the impact of β-dystroglycan deficiency on caveolin-1 and focal adhesion kinase (FAK), we analyzed the subcellular distribution of transfected and differentiated Meg-01 cells with confocal microscopy to detect caveolin-1 and FAK. The images corresponding to caveolin-1 showed a more intense label at the plasma membrane of RNAi transfected cells (Fig. 6A) while FAK images showed an accumulation of the label in the cytoplasm of these same cells (Fig. 6B). The overexpression of caveolin-1 and focal adhesion kinase (FAK) was quantified showing a significant increase (Fig. 6A and B). It is important to mention that after exposure to TPA to differentiate Meg01 cells, the cytoplasmic blebs were evident and the shape of the nucleus became irregular.

We next corroborated the consequences of β-dystroglycan depletion on the relative expression level of caveolin-1 and focal adhesion kinase by western blotting. Our results showed a significant overexpression of caveolin-1 and FAK in RNAi transfected cells compared to RNAi control cells (Fig. 6C). These results were confirmed by qRT-PCR assays (Fig. 6D)

DISCUSSION

Lipid rafts represent detergent insoluble membrane fractions enriched in cholesterol that are isolated from low-density matrices upon gradient centrifugation and are critical for many cellular functions. In platelets, lipid rafts have been implicated in activation and with the interaction to damaged endothelium [Brouckova and Holada, 2009; Munday et al., 2010]. In the present work we used caveolin-1 as a marker of rafts, however, after raft disruption by MβCD cholesterol depletion, thrombin-activated platelet caveolin-1, and flotilin-1 were enriched in the low-density fractions of the gradient and not only in the high-density ones. Our results using filipin, demonstrated that in MβCD-treated platelets cholesterol label was retained at the open canalicular system (OCS). This peculiar platelet structure is topologically similar to the plasma membrane as it possesses both an extracellular and a cytosolic face [Fitch-Tewfik and Flaumenhaft, 2013] where granules are centralized to release their contents into the OCS and diffuse out into the extracellular environment [Escolar and White, 1991]. These findings strongly suggest that MβCD had effect on some cholesterol pools but others are translocated to the rafts fractions upon activation to help to maintain and perform platelet functions.

The platelet membrane/lipid rafts (MLR), are scaffolds for many molecular entities that communicate extracellular stimuli to the intracellular milieu [Bodin et al., 2001]. The organization and/or the clustering of MLR into more active signalling platforms depend upon interactions with the dynamic cytoskeleton. Erythroblast enucleation [Konstantinidis et al., 2012], activation or interactions of platelets with damaged endothelial cells [Brouckova and Holada, 2009; Munday et al., 2010], as well as T-cell activation [Lin et al., 2010] are examples that illustrate the dependence of MLR-cytoskeletal interaction in blood cells. In addition to this evidence, our immunofluorescence images of cholesterol depleted platelets showed an important impact on filopodia extrusion of thrombin-activated platelets as well as on the typical full-spread morphology displayed during the adhesion process. In the present study, cytoskeleton-MLR interaction was evidenced with the presence of actin and tubulin in the raft fractions (Fig. 2A,B) and with their co-localisation with caveolin-1 according to respective confocal images (Fig. 2C,D). It is important to mention that the feasible association of Caveolin-1 PY14 with actin and tubulin observed by confocal analysis was further tested by Immunoprecipitation assay, a more rigorous analysis. We confirmed an interaction of Caveolin-1 PY14 with actin and desmin. A feasible association of caveolin-1 with tubulin could be established indirectly, mediated by actin as these two proteins have different interaction patterns [Selden and Pollard, 1986; Cerecedo et al., 2008; Cerecedo et al., 2013].

The platelet contractile proteins are one of the more thoroughly characterized non-muscle contractile systems and may be central to platelet hemostatic function [Pollard, 1977], including the granules content release [Nachman and Ferris, 1974], aggregation [Puszkin et al., 1977], and clot retraction [Pollard, 1977]; focal adhesions also referred to as focal contacts are essential sensors of the platelet tension generated during the adhesion process [Hagmann, 1993].

Caveolin-1 interacts with integrins [Wary et al., 1998] and has been shown to regulate focal adhesion domain organization, dynamics, and turnover [Goetz et al., 2008]. The distribution of caveolin-1 PY14 to platelet membrane protrusions is in agreement with observations in tumoral cells [Joshi et al., 2008] where it participates in cell signaling and actin reorganization upon integrin ligation in focal adhesions [del Pozo et al., 2005; Radel and Rizzo, 2005]. Our data did not show a direct interaction between Caveolin-1 PY14 with integrin β1, however, we have described the association of integrin β-1 with β-dystroglycan in adhered platelets [Cerecedo et al., 2008] suggesting that Caveolin-1 PY14 might regulate focal adhesions exerting its function through this last protein.

On the other hand, vinculin is essential for focal adhesions, as it interconnects with α-actinin and yields the bonding of the integrin β1 with the filamentous-actin cytoskeleton [Humphries et al., 2007; Ziegler et al., 2008]. Since platelets are not motile cells, we speculate that Caveolin-1 PY14 binding to vinculin might be cooperating to

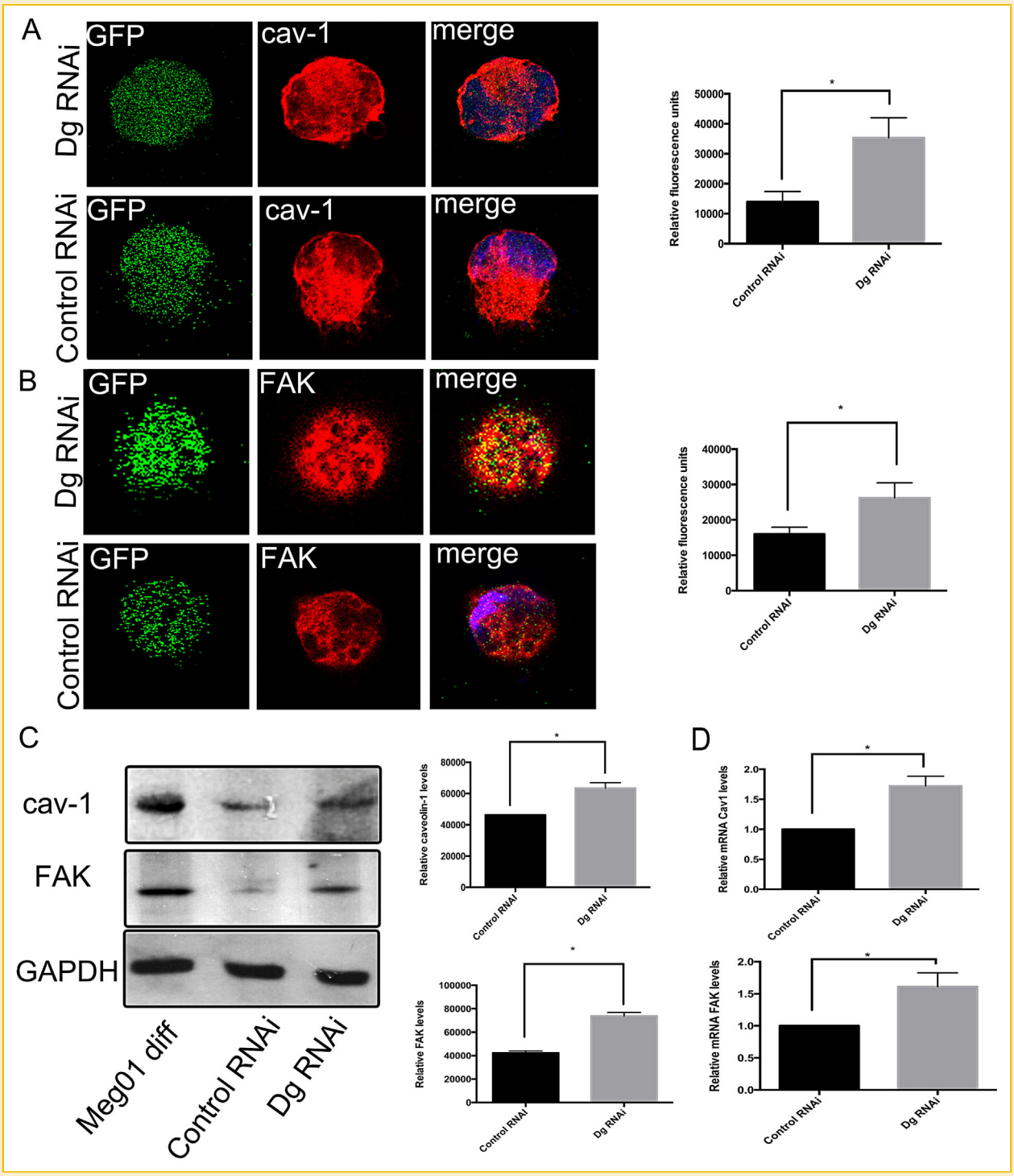

Fig. 6. β-dystroglycan depletion alters distribution and expression of caveolin-1 and focal adhesion kinase (FAK). Panel A. Meg-01 cells expressing either control RNAi or Dg RNAi were immunolabeled for caveolin-1 and analyzed for confocal microscopy. Relative fluorescence units showed a significant caveolin-1 up-regulation. Values shown are mean ± SEM from three independent experiments (n = 3). $^{*}P < 0.005$. Panel B. Meg-01 cells expressing either control RNAi or Dg RNAi were immunolabeled for focal adhesion kinase (FAK) and analyzed for confocal microscopy. Relative fluorescence units showed a significant FAK overexpression. Values shown are mean ± SD from three independent experiments (n = 3). $^{*}P < 0.005$. Panel C. Meg-01 differentiated cells extracts, total Meg-01 cells extracts expressing either control RNAi or Dg RNAi were processed for western blot, utilizing an antibody against caveolin-1, and focal adhesion kinase (FAK). Densitometry analysis demonstrated caveolin-1 and focal adhesion kinase (FAK) overexpression in cells transfected with a Dg RNAi as compared with cells transfected with a control RNAi. Values shown are mean ± SD from three independent experiments (n = 3), respectively. $^{*}P < 0.005$. Panel D. Messenger RNA-expression of caveolin-1 and FAK was examined by quantitative reverse transcription PCR in RNAi control and RNAi Dg. Values shown are mean ± SEM from three independent experiments (n = 3), respectively. $P < 0.05$.

slow or limit the exchange of FAK, increasing the stability of these proteins in focal adhesions domains and promoting its maturation [Goetz et al., 2008].

Dystroglycan is a multifunctional scaffold involved in adhesion and adhesion-mediated signalling in a multitude of cell types and tissues [Moore and Winder, 2010], and is known to interact with other caveolin family members [Sotgia et al., 2000]. Our data strongly suggest that disruption of β-dystroglycan interaction with caveolin-1 after cholesterol depletion impairs platelet functions as has been demonstrated in other systems [Sharma et al., 2010; Vega-Moreno et al., 2012; Palma-Flores et al., 2014]. The interaction between caveolin-1 and β-dystroglycan appears to have a functional role, because in β-dystroglycan depleted platelet progenitors, caveolin-1 and FAK were up-regulated and accumulated at the plasma membrane and cytoplasm respectively, suggesting that the interaction of caveolae with structural proteins and actin cytoskeleton supports modulation of signalling molecules and adhesion process.

At this point, we tempted to state that caveolin-1 in association with vinculin and β-dystroglycan provide platforms that increase the local concentration of the signaling molecules contributing to the hemostasis. Specifically participating in the consolidation of the adhesion of platelets to sites of vessel damage to clot formation and transmitting the corresponding intracellular signals.

Plasma membrane lipid microdomains are regulated by the formation of sites of cellular adhesion to the surrounding matrix, which mechanically couples to the actin cytoskeleton (so-called focal complexes/adhesions) [Sargiacomo et al., 1995]. Adhesion mechanisms may direct the formation of lipid domains and direct the endocytosis of specific ligands from specific regions of the plasma membrane; suggesting that the formation of local adhesive structures is instrumental in the mechanism of internalization [Allen and Aderem, 1996]. Platelets can ingest small particles but when they are too large such as bacteria platelets behave as covercytes but not phagocytes and the OCS (open canalicular system) is critically involved in spreading on any surface as has been described [White, 2005].

Our study demonstrates the indispensable interaction of caveolin-1 with the cytoskeleton, which includes shape change and adhesion. Caveolin-1 PY14 modulates the focal adhesion complex through vinculin and participates in the tension forces exerted during adhesion and clot retraction. Additionally, our results are indicative of β-dystroglycan key role in platelet adhesion as we demonstrate that it is compensated with caveolin-1 and FAK up-regulation.

ACKNOWLEDGMENTS

This work was supported by CONACYT-México, grant no.167178

Conflict of interest

All the authors stated that they do not have any conflict of interest.

REFERENCES

Allen LA,Aderem A. 1996. Mechanisms of phagocytosis. Curr Opin Immunol 8:36–40.

Bearer EL, Prakash JM, Li Z. 2002. Actin dynamics in platelets. Int Rev Cytol 217:137–182.

Bodin S, Soulet C, Tronchere H, Sie P, Gachet C, Plantavid M, Payrastre B. 2005. Integrin-dependent interaction of lipid rafts with the actin cytoskeleton in activated human platelets. J Cell Sci 118:759–769.

Bodin S, Giuriato S, Ragab J, Humbel BM, Viala C, Vieu C, Chap H, Payrastre B. 2001. Production of phosphatidylinositol 3,4,5-trisphosphate and phosphatidic acid in platelet rafts: Evidence for a critical role of cholesterol-enriched domains in human platelet activation. Biochemistry 40:15290–15299.

Brouckova A, Holada K. 2009. Cellular prion protein in blood platelets associates with both lipid rafts and the cytoskeleton. Thromb Haemost 102:966–974.

Castanho MA, Coutinho A, Prieto MJ. 1992. Absorption and fluorescence spectra of polyene antibiotics in the presence of cholesterol. J Biol Chem 267:204–209.

Cerecedo D, Cisneros B, Suarez-Sanchez R, Hernandez-Gonzalez E, Galvan I. 2008. Beta-Dystroglycan modulates the interplay between actin and microtubules in human-adhered platelets. Br J Haematol 141:517–528.

Cerecedo D, Martinez-Vieyra I, Mondragon R, Mondragon M, Gonzalez S, Galvan IJ. 2013. Haemostatic role of intermediate filaments in adhered platelets: Importance of the membranous system stability. J Cell Biochem 114:2050–2060.

Cerecedo D, Martinez-Rojas D, Chavez O, Martinez-Perez F, Garcia-Sierra F, Rendon A, Mornet D, Mondragon R. 2005. Platelet adhesion: Structural and functional diversity of short dystrophin and utrophins in the formation of dystrophin-associated-protein complexes related to actin dynamics. Thromb Haemost 94:1203–1212.

del Pozo MA, Balasubramanian N, Alderson NB, Kiosses WB, Grande-Garcia A, Anderson RG, Schwartz MA. 2005. Phospho-caveolin-1 mediates integrin-regulated membrane domain internalization. Nat Cell Biol 7: 901–908.

Escolar G, White JG. 1991. The platelet open canalicular system: a final common pathway. Blood Cells 17:467–485.discussion 486-495.

Fitch-Tewfik JL, Flaumenhaft R. 2013. Platelet granule exocytosis: A comparison with chromaffin cells. Front Endocrinol (Lausanne) 4:77.

Glenney JR, Jr. 1989. Tyrosine phosphorylation of a 22-kDa protein is correlated with transformation by Rous sarcoma virus. J Biol Chem 264:20163–20166.

Goetz JG, Joshi B, Lajoie P, Strugnell SS, Scudamore T, Kojic LD, Nabi IR. 2008. Concerted regulation of focal adhesion dynamics by galectin-3 and tyrosine-phosphorylated caveolin-1. J Cell Biol 180:1261–1275.

Gonnord P, Blouin CM, Lamaze C. 2012. Membrane trafficking and signaling: Two sides of the same coin. Semin Cell Dev Biol 23:154–164.

Hagmann J. 1993. Pattern formation and handedness in the cytoskeleton of human platelets. Proc Natl Acad Sci USA 90:3280–3283.

Head BP, Insel PA. 2007. Do caveolins regulate cells by actions outside of caveolae? Trends Cell Biol 17:51–57.

Humphries JD, Wang P, Streuli C, Geiger B, Humphries MJ, Ballestrem C. 2007. Vinculin controls focal adhesion formation by direct interactions with talin and actin. J Cell Biol 179:1043–1057.

Ilsley JL, Sudol M, Winder SJ. 2001. The interaction of dystrophin with beta-dystroglycan is regulated by tyrosine phosphorylation. Cell Signal 13:625–632.

Ilsley JL, Sudol M, Winder SJ. 2002. The WW domain: Linking cell signalling to the membrane cytoskeleton. Cell Signal 14:183–189.

James M, Nuttall A, Ilsley JL, Ottersbach K, Tinsley JM, Sudol M, Winder SJ. 2000. Adhesion-dependent tyrosine phosphorylation of (beta)-dystroglycan regulates its interaction with utrophin. J Cell Sci 113(Pt10):1717–1726.

Joshi B, Bastiani M, Strugnell SS, Boscher C, Parton RG, Nabi IR. 2012. Phosphocaveolin-1 is a mechanotransducer that induces caveola biogenesis via Egr1 transcriptional regulation. J Cell Biol 199:425–435.

Joshi B, Strugnell SS, Goetz JG, Kojic LD, Cox ME, Griffith OL, Chan SK, Jones SJ, Leung SP, Masoudi H, Leung S, Wiseman SM, Nabi IR. 2008. Phosphorylated caveolin-1 regulates Rho/ROCK-dependent focal adhesion dynamics and tumor cell migration and invasion. Cancer Res 68:8210–8220.

Konstantinidis DG, Pushkaran S, Johnson JF, Cancelas JA, Manganaris S, Harris CE, Williams DA, Zheng Y, Kalfa TA. 2012. Signaling and cytoskeletal requirements in erythroblast enucleation. Blood 119:6118–6127.

Li S, Seitz R, Lisanti MP. 1996. Phosphorylation of caveolin by src tyrosine kinases. The alpha-isoform of caveolin is selectively phosphorylated by v-Src in vivo. J Biol Chem 271:3863–3868.

Lin SL, Chien CW, Han CL, Chen ES, Kao SH, Chen YJ, Liao F. 2010. Temporal proteomics profiling of lipid rafts in CCR6-activated T cells reveals the integration of actin cytoskeleton dynamics. J Proteome Res 9:283–297.

Martinez-Zarate AD, Martinez-Vieyra I, Alonso-Rangel L, Cisneros B, Winder SJ, Cerecedo D. 2014. Dystroglycan depletion inhibits the functions of differentiated HL-60 cells. Biochem Biophys Res Commun 448:274–280.

Mitchell A, Mathew G, Jiang T, Hamdy FC, Cross SS, Eaton C, Winder SJ. 2013. Dystroglycan function is a novel determinant of tumor growth and behavior in prostate cancer. Prostate 73:398–408.

Moore CJ, Winder SJ. 2010. Dystroglycan versatility in cell adhesion: A tale of multiple motifs. Cell Commun Signal 8:3.

Munday AD, Gaus K, Lopez JA. 2010. The platelet glycoprotein Ib-IX-V complex anchors lipid rafts to the membrane skeleton: Implications for activation-dependent cytoskeletal translocation of signaling molecules. J Thromb Haemost 8:163–172.

Nachman RL, Ferris B. 1974. Binding of adenosine diphosphate by isolated membranes from human platelets. J Biol Chem 249:704–710.

Nachmias VT. 1980. Cytoskeleton of human platelets at rest and after spreading. J Cell Biol 86:795–802.

Ogura M, Morishima Y, Okumura M, Hotta T, Takamoto S, Ohno R, Hirabayashi N, Nagura H, Saito H. 1988. Functional and morphological differentiation induction of a human megakaryoblastic leukemia cell line (MEG-01s) by phorbol diesters. Blood 72:49–60.

Palma-Flores C, Ramirez-Sanchez I, Rosas-Vargas H, Canto P, Coral-Vazquez RM. 2014. Description of a utrophin associated protein complex in lipid raft domains of human artery smooth muscle cells. Biochim Biophys Acta 1838:1047–1054.

Pollard TD. 1977. Actin, myosin and cofactor from motile cells. J Mechanochem Cell Motil 4:15–30.

Puszkin EG, Maldonado R, Spaet TH, Zucker MB. 1977. Platelet myosin. Localization of the rod myosin fragment and effect of its antibodies on platelet function. J Biol Chem 252:4371–4378.

Radel C, Rizzo V. 2005. Integrin mechanotransduction stimulates caveolin-1 phosphorylation and recruitment of Csk to mediate actin reorganization. Am J Physiol Heart Circ Physiol 288:H936–H945.

Salanueva IJ, Cerezo A, Guadamillas MC, del Pozo MA. 2007. Integrin regulation of caveolin function. J Cell Mol Med 11:969–980.

Sargiacomo M, Scherer PE, Tang Z, Kubler E, Song KS, Sanders MC, Lisanti MP. 1995. Oligomeric structure of caveolin: Implications for caveolae membrane organization. Proc Natl Acad Sci USA 92:9407–9411.

Sechi AS, Wehland J. 2000. The actin cytoskeleton and plasma membrane connection: PtdIns(4,5)P(2) influences cytoskeletal protein activity at the plasma membrane. J Cell Sci 113(Pt21):3685–3695.

Selden SC, Pollard TD. 1986. Interaction of actin filaments with microtubules is mediated by microtubule-associated proteins and regulated by phosphorylation. Ann NY Acad Sci 466:803–812.

Seveau S, Eddy RJ, Maxfield FR, Pierini LM. 2001. Cytoskeleton-dependent membrane domain segregation during neutrophil polarization. Mol Biol Cell 12:3550–3562.

Sharma P, Ghavami S, Stelmack GL, McNeill KD, Mutawe MM, Klonisch T, Unruh H, Halayko AJ. 2010. Beta-Dystroglycan binds caveolin-1 in smooth muscle: A functional role in caveolae distribution and Ca2+ release. J Cell Sci 123:3061–3070.

Simons K, Gerl MJ. 2010. Revitalizing membrane rafts: New tools and insights. Nat Rev Mol Cell Biol 11:688–699.

Sotgia F, Lee JK, Das K, Bedford M, Petrucci TC, Macioce P, Sargiacomo M, Bricarelli FD, Minetti C, Sudol M, Lisanti MP. 2000. Caveolin-3 directly interacts with the C-terminal tail of beta -dystroglycan. Identification of a central WW-like domain within caveolin family members. J Biol Chem 275:38048–38058.

Vega-Moreno J, Tirado-Cortes A, Alvarez R, Irles C, Mas-Oliva J, Ortega A. 2012. Cholesterol depletion uncouples beta-dystroglycans from discrete sarcolemmal domains, reducing the mechanical activity of skeletal muscle. Cell Physiol Biochem 29:905–918.

Villalba M, Bi K, Rodriguez F, Tanaka Y, Schoenberger S, Altman A. 2001. Vav1/Rac-dependent actin cytoskeleton reorganization is required for lipid raft clustering in T cells. J Cell Biol 155:331–338.

Viola A, Gupta N. 2007. Tether and trap: Regulation of membrane-raft dynamics by actin-binding proteins. Nat Rev Immunol 7:889–896.

Wary KK, Mariotti A, Zurzolo C, Giancotti FG. 1998. A requirement for caveolin-1 and associated kinase Fyn in integrin signaling and anchorage-dependent cell growth. Cell 94:625–634.

White JG. 1999. Platelet membrane interactions. Platelets 10:368–381.

White JG. 2005. Platelets are covercytes, not phagocytes: Uptake of bacteria involves channels of the open canalicular system. Platelets 16:121–131.

Ziegler WH, Gingras AR, Critchley DR, Emsley J. 2008. Integrin connections to the cytoskeleton through talin and vinculin. Biochem Soc Trans 36: 235–239.

SUPPORTING INFORMATION

Additional supporting information may be found in the online version of this article at the publisher's web-site.